ELSEVIER

Surface Science 307–309 (1994) 907–911

surface science

Coherence versus incoherence of photoemission and Auger signals at resonance

M.F. López, C. Laubschat, A. Gutiérrez, E. Weschke, A. Höhr, M. Domke, G. Kaindl *

Institut für Experimentalphysik, Freie Universität Berlin, Arnimallee 14, D14195 Berlin-Dahlem, Germany

(Received 20 August 1993)

Abstract

A comparative resonant photoemission (PE) study of Ni, Fe and Eu metal as well as Ce in CeGd is reported. It is shown that the resonant enhancement of the 6 eV satellite in the valence-band PE spectrum of Ni metal is almost completely due to an incoherent superposition of the valence-band PE spectrum with an intense Auger emission signal. On the other hand, the resonant enhancement of 4f signals from rare-earth systems turns out to be a true resonant PE phenomenon.

In the past two decades, resonant photoemission (PE) has been developed as a powerful tool for the study of the correlated electronic structure of 3d-transition-metal, rare-earth and actinide systems [1–14]. The phenomenon is based on an interference between the direct PE channel and the dipole transition of a core electron to a discrete unoccupied state, occurring at energies close to a particular absorption threshold; it gives rise to strong variations of the PE cross section. On the other hand, the competing non-coherent Coster–Kronig decay of the core-excited state leads to the emission of Auger electrons, which have the same kinetic energy as photoelectrons excited at resonance. This makes a distinction between resonant PE and a non-coherent Auger decay process rather difficult. A clear distinction between the two processes, however, is of crucial interest for a proper interpretation of the observed spectral structures. Although this problem had already been addressed about 14 years ago in connection with the resonant enhancement of the well-known 6 eV correlation satellite in the valence-band PE spectrum of Ni metal [15], it was subsequently completely ignored in resonant PE studies; only very recently has the issue been addressed again [16].

In the present publication, we present the results of a systematic comparison of resonant electron-emission processes at the L_{III} and M_{III} thresholds of 3d transition metals with those occurring at the M_V and $N_{IV,V}$ thresholds of rare-earth systems. It turns out that only in the case of rare-earth systems, the observed resonance phenomena represent true resonant PE processes, while in case of 3d-transition-metal systems, they are governed by intense non-coherent Auger de-

* Corresponding author.

SSDI 0039-6028(93)E0829-J

cay processes. In particular, the resonant enhancement of the 6 eV Ni satellite is predominantly due to a non-coherent superposition of the valence-band PE spectrum with an intense Auger emission signal. This is concluded from a careful analysis of valence-band PE spectra of Fe and Ni metal at and above the $2p \rightarrow 3d$ absorption threshold as well as by the results of angle-dependent PE studies at the Ni $3p \rightarrow 3d$-resonance. A comparison with resonant PE data for Eu metal at the $3d \rightarrow 4f$-resonance and for CeGd at the Ce $4d \rightarrow 4f$-resonance reveals that – in contrast to the case of 3d metals – the intensity enhancement in rare-earth systems reflects a true resonant PE process.

The experiments were performed at the SX700/II, KMC, and TGM1 beamlines of the Berliner Elektronenspeicherring für Synchrotronstrahlung (BESSY), employing various hemispherical electron-energy analyzers. The angle-resolved measurements were performed with an angular acceptance cone of $\pm 2°$. Polycrystalline samples were cleaned in situ by scraping with a diamond file. Oxygen contaminations were checked by monitoring the O 2p PE signal at $h\nu = 40$ eV or the O 1s PE signal at $h\nu = 900$ eV, respectively, and were found to be negligible. During the experiments, the pressure in the experimental chamber did not exceed 2×10^{-10} mbar.

Fig. 1 shows comparative PE spectra of polycrystalline Fe and Eu metal taken in the photon-energy regions of the L_{III} and M_V resonances, respectively. The different behaviors of the more band-like 3d metal, displayed on the right panel and the localized 4f system, displayed on the left panel, are obvious. For Eu metal, the intensity of the Eu $4f^6\ ^7F$ multiplet at $\simeq 2$ eV BE is strongly enhanced at resonance ($h\nu = 1123.3$ eV), while its position, indicated by the solid vertical bars, does not change. For higher photon energies, the intensity of the 4f emission decreases, but no Auger signal can be identified. Note, that the weak structure at about 6 eV BE, visible in the spectra at $h\nu = 1127.3$ eV and $h\nu = 1129.3$ eV, reflects emission to a ^5X final state [17].

In contrast, the corresponding PE spectra of Fe metal reveal the presence of a strong Auger

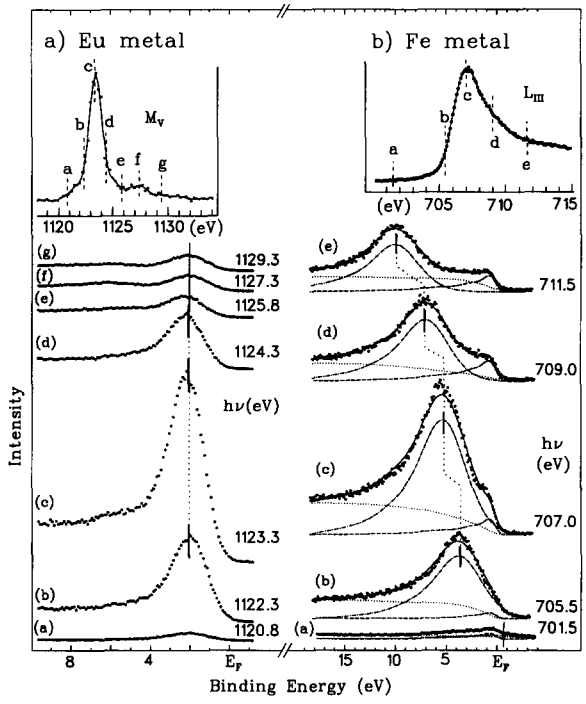

Fig. 1. (a) Photon-excited electron spectra of Eu metal taken at the given photon energies in the region of the M_V resonance. (b) Photon-excited electron spectra of Fe metal taken at the given photon energies in the region of the L_{III} resonance. In the Fe-metal spectra, the solid lines through the data points represent the results of least-squares fits (see text), with the dashed subspectra representing the PE signal and the dash-dotted subspectra the Coster–Kronig Auger contributions. The Eu M_V and Fe L_{III} XANES spectra, respectively, measured in total electron yield, are given in the insets. The dashed vertical bars indicate the photon energies at which the individual spectra were recorded.

signal at photon energies above threshold. Here, the seeming resonant enhancement of the spectral intensity in the valence-band PE region is simply due to the non-coherent superposition of a strong $L_3M_{4,5}M_{4,5}$ Auger signal and a weak valence-band PE spectrum. The intensity of the Auger signal is highest for $h\nu = 707$ eV due to the enhanced creation of a $2p_{3/2}$ core hole at resonance. To check the validity of this interpretation, the data were least-squares fitted by a superposition of two components representing the Auger and PE valence-band emission; the shapes of these components were derived from Auger

and PE spectra taken far from resonance. The solid lines through the data points represent the results of this analysis. The dashed and dash-dotted subspectra represent the Auger and PE components, respectively, and the dotted curve reflects the background contribution of inelastically scattered electrons. As is obvious from Fig. 1, the description of the spectra within this simple model is rather successful; the small misfit at $\simeq 6$ eV BE in the $h\nu = 707$ eV spectrum can be ascribed either to the resonant enhancement of a possible satellite [18–22] or to a small change in the shape of the Auger spectrum in the resonance region.

Analogous experiments were performed for Ni metal, the electronic structure of which is known to be at the border between band-like and localized behavior. The resulting PE spectra, analyzed like in the Fe case, are presented in Fig. 2. The valence-band PE spectra of Ni metal are characterized by a satellite structure 6 eV below the Fermi level, E_F, which cannot be explained by a single-particle density of states, but is a signature of a $3d^8$ two-hole final state [6–9]. For photon energies in the region of the M_{III} absorption resonance, this satellite is resonantly enhanced, while the $3d^9$ valence-band PE spectrum is almost unaffected by the resonance process. The solid lines through the data points, as well as the subspectra, are again the results of a least-squares fit analysis, as in the Fe-metal case. The dominant resonance contribution to the spectra originates from $L_3M_{4,5}M_{4,5}$ Auger emission, as in Fe metal; in contrast, however, a resonant enhancement of the 6 eV PE satellite by a factor of 12 had to be included for a good description of the data. Here, again the question arises whether this increase in the intensity of the satellite reflects a resonant PE phenomenon or – as in case of the misfit of the Fe-metal spectrum – simply a change in the spectral shape of the Auger signal.

Even in case of Eu metal, a possible Auger contribution cannot be ruled out on the basis of spectral shapes alone. If it would only occur at M_V resonance, where the cross section for core-hole production is resonantly enhanced, its energy would coincide with the PE signal. This question, however, can be addressed by measuring the intensity of the various spectral components as a function of the electron emission angle relative to the E-vector of the incident light. In the case of a PE process, the intensity should show a $\cos^2$ behaviour, while an Auger signal ought to be isotropic in case of a polycrystalline sample. On the basis of these arguments, a distinction between PE and Auger contributions should be possible on the basis of angle-dependent electron-spectroscopy measurements.

To ensure better experimental resolution, the angle-resolved experiment was performed for Ni metal at the M_{III} absorption resonance instead of

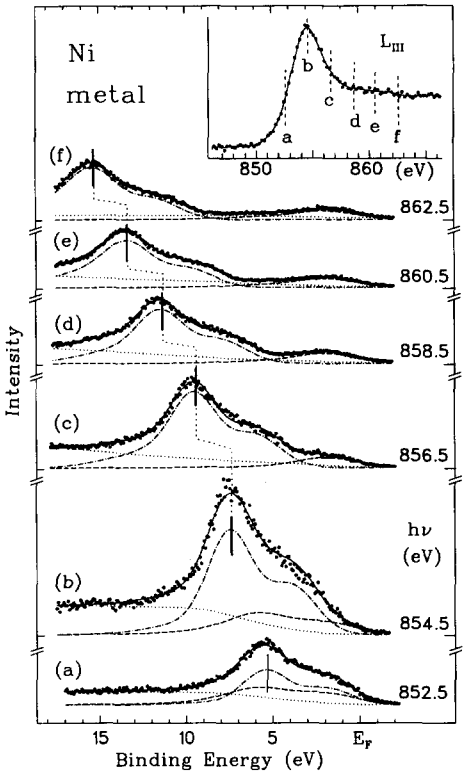

Fig. 2. Photon-excited electron spectra of Ni metal taken at the given photon energies. The solid lines through the data points represent the results of least-squares fits (see text), with the dashed subspectra representing the PE signals and the dash-dotted subspectra the Coster–Kronig Auger contributions. The dotted curves represent the integral backgrounds. The L_{III}-XANES spectrum is given in the inset; the dashed vertical bars indicate the photon energies at which the spectra (a) to (f) were recorded.

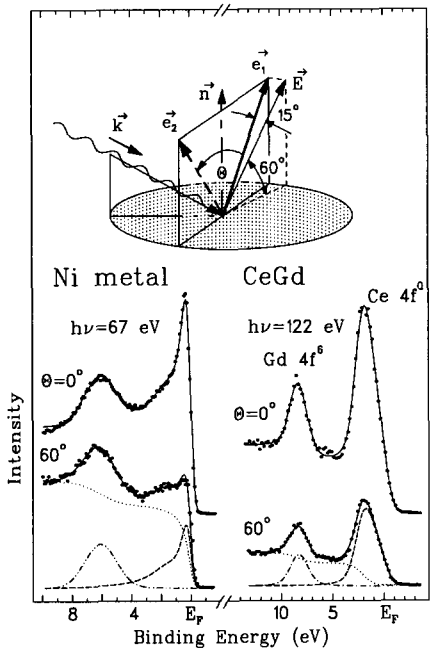

Fig. 3. On-resonance photoelectron spectra of Ni metal ($h\nu$ = 67 eV) and of CeGd ($h\nu$ = 122 eV) for two different angles Θ. For Ni metal, the solid lines through the data points represent the results of least-squares fits (see text): the dashed subspectrum represents the PE signal, and the dash-double-dotted curve the 6 eV satellite feature. In the CeGd spectra, the dash-dotted subspectrum represents the Gd 4f emission and the dashed subspectrum the on-resonance Ce 4f emission. The dotted curves describe integral backgrounds. The inset describes the geometry of the experiment: $\boldsymbol{E}$ and $\boldsymbol{k}$ represent the direction of the electric field vector and the photon momentum, respectively, $\boldsymbol{n}$ the surface normal and $\boldsymbol{e}_{1,2}$ the directions of electron emissions. This geometry was chosen to assure the same surface sensitivity for $\Theta = 0°$ and $\Theta = 60°$.

L_{III}. Fig. 3 (left panel) shows PE spectra of polycrystalline Ni metal, taken at $h\nu = 67$ eV (M_{III} resonance) for two different angles Θ. The experimental geometry with a definition of Θ is given in the inset of Fig. 3. The spectra were normalized to equal intensities of the $M_3M_{4,5}M_{4,5}$ Auger signals measured far from resonance [16]. As expected, the intensity of the valence-band emission close to E_F drops off roughly proportional to $\cos^2\Theta$, while that of the satellite stays constant. This means that the 6 eV satellite behaves almost entirely as an Auger signal, i.e. its seeming resonant enhancement is caused by the incoherent superposition with an Auger signal.

To ensure that the Auger-like angular character of the satellite emission is not a general property of resonant PE, Fig. 3 (right panel) shows PE spectra of the polycrystalline alloy GdCe, taken in Ce 4d → 4f-resonance at $h\nu = 122$ eV; the spectra were taken at the same angles Θ as those of Ni metal and the same normalization procedure was applied. At a BE of 2 eV, the resonantly enhanced emission from the Ce 4f states is observed, while the weaker emission at ≃ 8 eV BE represents non-resonant PE from Gd 4f states, which can be used for internal calibration. When increasing the angle Θ from 0° to 60°, the intensity of both resonant Ce 4f and non-resonant Gd 4f emissions decrease in exactly the same way, roughly proportional to $\cos^2\Theta$. These identical angular dependences follow directly from the ratio of intensities of the Ce 4f and Gd 4f PE signals, which obviously does not change from $\Theta = 0°$ to $\Theta = 60°$. This proves that the resonantly enhanced Ce 4f PE signal behaves according to a PE process.

In conclusion, we have shown that the resonant enhancement of the 6 eV satellite in the PE spectrum of Ni metal, both in the 3p → 3d and 2p → 3d-resonance regions, is almost completely due to a non-coherent superposition of the valence-band PE signal with the corresponding $M_3M_{4,5}M_{4,5}$ or $L_3M_{4,5}M_{4,5}$ Auger emission, respectively. This clear difference to the resonant PE behavior in rare-earth systems is probably caused by a weaker localization of the 3d states, where a strong hybridization of the dipole-excited state with the surrounding d-bands leads to delocalization and thereby to a loss of coherence.

The authors acknowledge the help of Dr. Miguel Abbate in the measurements on Fe metal and the general assistance by the staff of BESSY. This work was supported by the Bundesminister für Forschung und Technologie, project 05-5KEAXI-3/TP01 and the Deutsche Forschungsgemeinschaft, project Ka564/2-2. Two of the authors (M.F.L. and A.G.) thank the Spanish Ministerio de Educación y Ciencia for financial support.

1. References

[1] U. Fano, Phys. Rev. 124 (1961) 1866.
[2] C. Guillot, Y. Ballu, J. Paigné, J. Lecante, K.P. Jain, P. Thiry, R. Pinchaux, Y. Pétroff and L.M. Falicov, Phys. Rev. Lett. 39 (1977) 1632.
[3] Y. Sakisaka, T. Komeda, M. Onchi, H. Kato, S. Masuda and K. Yagi, Phys. Rev. B 36 (1987) 6383.
[4] O. Björneholm, J.N. Andersen, C. Wigren, A. Nilsson, R. Nyholm and N. Mårtensson, Phys. Rev. B 41 (1990) 10408.
[5] J. Barth, G. Kalkoffen and C. Kunz, Phys. Lett. 74A (1979) 360.
[6] T. Jo, A. Kotani, J.C. Parlebas and J. Kanamori, J. Phys. Soc. Jpn. 52 (1983) 2581.
[7] D.R. Penn, Phys. Rev. Lett. 42 (1979) 921.
[8] A. Liebsch, Phys. Rev. Lett. 43 (1979) 1431; Phys. Rev. B 23 (1981) 5203.
[9] L.C. Davis and L.A. Feldkamp, Phys. Rev. B 23 (1981) 6239.
[10] S.M. Girvin and D.R. Penn, Phys. Rev. B 22 (1980) 4081.
[11] J.C. Parlebas, A. Kotani and J. Kanamori, J. Phys. Soc. Jpn. 51 (1982) 124.
[12] C. Laubschat, E. Weschke, G. Kalkowski and G. Kaindl, Phys. Scr. 41 (1990) 124.
[13] L.H. Tjeng, C.T. Chen, J. Chijsen, P. Rudolf and F. Sette, Phys. Rev. Lett. 67 (1991) 501.
[14] G. van der Laan, B.T. Thole, H. Ogasawara, Y. Seino and A. Kotani, Phys. Rev. B 46 (1992) 7221.
[15] M.M. Traum, N.V. Smith, H.H. Farrell, D.P. Woodruff and D. Norman, Phys. Rev. B 20 (1979) 4008.
[16] M.F. López, A. Höhr, C. Laubschat, M. Domke and G. Kaindl, Europhys. Lett. 20 (1992) 357;
M.F. López, C. Laubschat, A. Gutiérrez, E. Weschke, M. Domke and G. Kaindl, preprint (1993).
[17] C. Laubschat, E. Weschke, G. Kalkowski and G. Kaindl, Phys. Scr. 41 (1990) 124.
[18] H. Kato, T. Ishii, S. Masuda, Y. Harada, T. Miyano, T. Komeda, M. Onchi and Y. Sakisaka, Phys. Rev. B 32 (1985) 1992.
[19] K.H. Walker, E. Kisker, C. Carbone and R. Clauberg, Phys. Rev. B 35 (1987) 1616.
[20] S. Raaen and V. Murgai, Phys. Rev. B 36 (1987) 887.
[21] K. Schröder, E. Kisker and A. Bringer, Solid State Commun. 55 (1985) 377.
[22] D. Chandesris, J. Lecante and Y. Pétroff, Phys. Rev. B 27 (1983) 2630.